Proceedings of the International Symposium on Engineering Lessons Learned from
the 2011 Great East Japan Earthquake, March 1-4, 2012, Tokyo, Japan

# EVALUATION OF STRONG GROUND MOTIONS OF THE 2011 GREAT EAST JAPAN EARTHQUAKE BASED ON NONLINEAR RESPONSE OF STANDARD BRIDGES

Hiroshi MATSUZAKI[1] and Kazuhiko KAWASHIMA[2]

[1] Assistant Professor, Department of Civil Engineering, Tokyo Institute of Technology, Tokyo, Japan, matsuzaki.h.aa@m.titech.ac.jp
[2] Professor, ditto, kawashima.k.ae@m.titech.ac.jp

**ABSTRACT**: Intensities of ground motions recorded during the 2011 Great East Japan earthquake is evaluated based on nonlinear seismic response of three bridges. It is shown that response under JMA Furukawa ground motion develops the largest response among the ground motions recoded during the 2011 Great East Japan earthquake, however it is smaller than the response under JR Takatori ground motion recorded during the 1995 Kobe earthquake. It is also noted that high PGA ground motions such as K-net Tsukidate ground motions do not produce large response of the bridges.

**Key Words**: Intensity, Strong Ground Motions, Bridges, Nonlinear Response

## INTRODUCTION

Ground-motion-induced damage was limited to the bridges which were designed in accordance with the post-1990 design codes (JSCE 2011, Kawashima 2012). It is considered that the intensity of ground motions during the 2011 Great East Japan earthquake was smaller than the Type I and II design ground motions in the post-1990 design codes as shown in Fig. 1. The Type I and II design ground

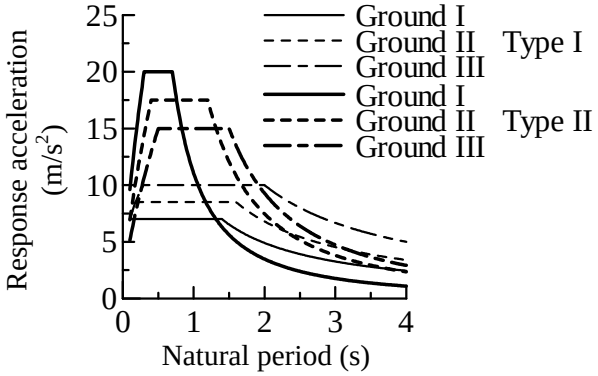


Fig. 1 Type I and II design ground motions

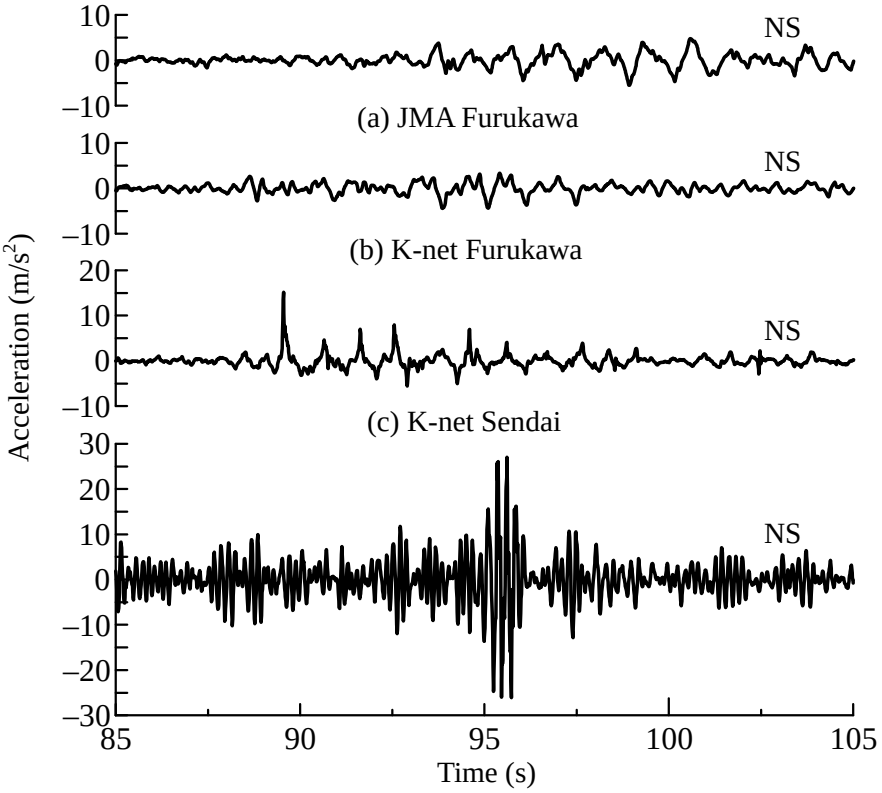


Fig. 2 Ground accelerations recorded during the 2011 Great East Japan earthquake

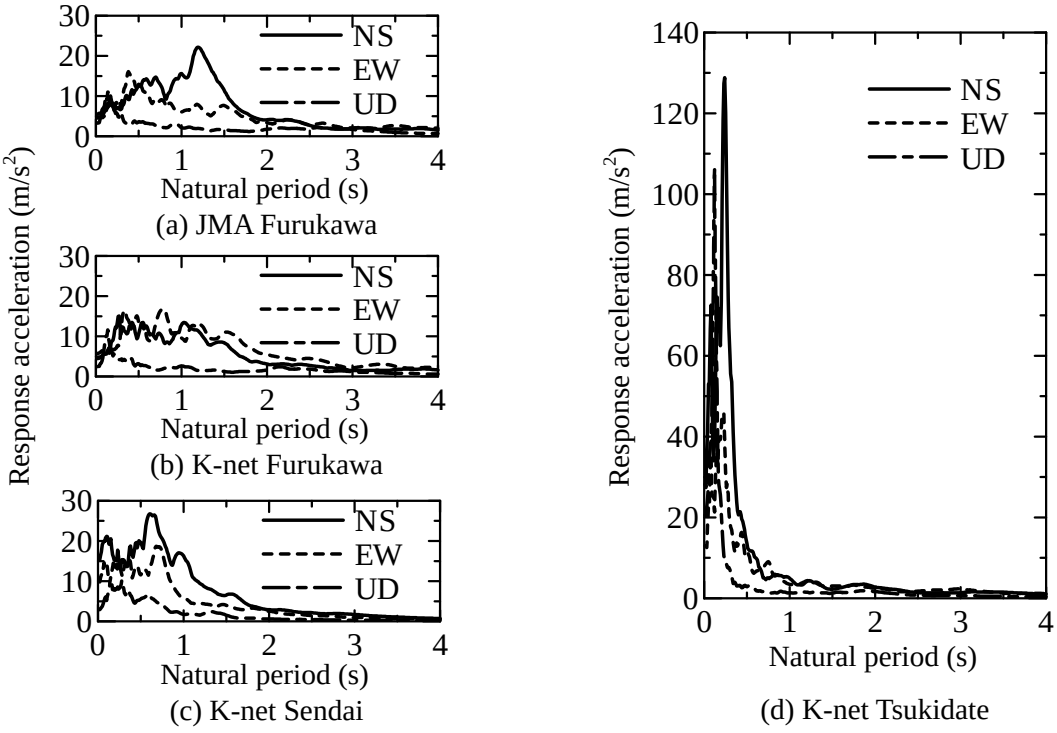


Fig. 3 Response acceleration spectra of ground motions during the 2011 Great East Japan earthquake

motions were set so that they represent ground motions which possibly developed at Tokyo during the 1923 Great Kanto earthquake and the ground motions recorded during the 1995 Kobe earthquake (JRA

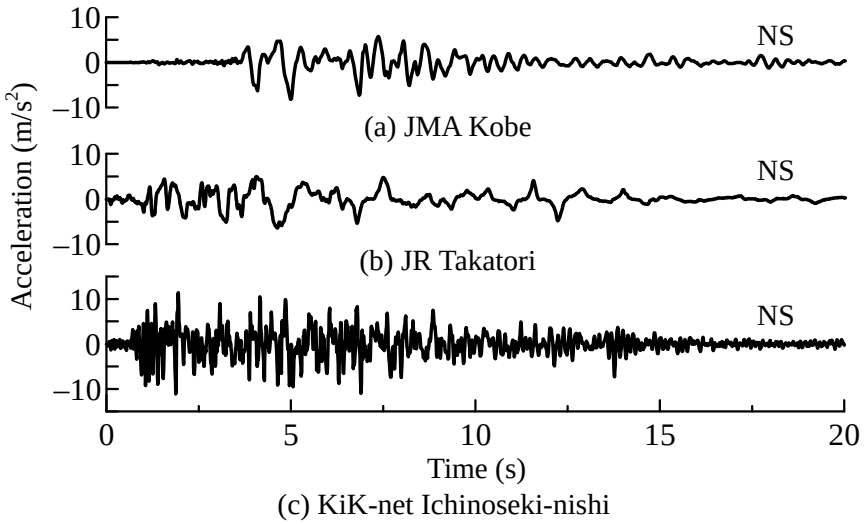

(c) KiK-net Ichinoseki-nishi

Fig. 4 Ground accelerations recorded during the 1995 Kobe earthquake and the 2008 Iwate-Miyagi earthquake

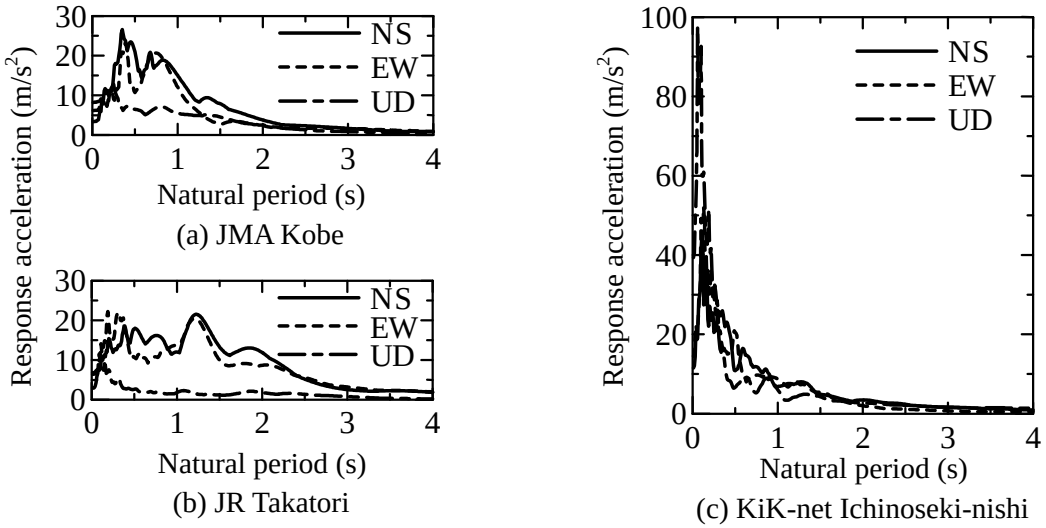


Fig. 5 Response acceleration spectra of ground motions recorded during the 1995 Kobe earthquake and the 2008 Iwate-Miyagi earthquake

1996 and 2002, Kawashima 2000).

Figs. 2 and 3 shows some typical ground accelerations recorded at K-net and JMA sites during the 2011 Great East Japan earthquake and their acceleration response spectra. Though duration was over 300s, only the accelerations for 20s including the peak are shown here. It should be noted here that since only few K-net and JMA sites were resting on soft soil sites with majority sites being on stiff sites, direct comparison with the design ground motions cannot be meaningful. At the stiff sites, some ground accelerations had very high response accelerations at short period range (less than 0.4s), but they had response values less than 10m/s$^2$ at period over 1s.

For examples, the ground acceleration at K-net Tsukidate (refer to Fig. 2) had a PGA of 27 m/s$^2$ leading to a 129m/s$^2$ response acceleration at 0.24s. JMA intensity was 7 in this city. However almost no structural damage occurred in engineering structures here. This clearly shows that high PGA due to high frequency spike is not absolutely important for structural design for bridges. From this sense, the ground motions recorded during the Great East Japan earthquake was not destructive to engineering structures.

However it should be noted that at soft soil sites such as Osaki City (JMA Furukawa and K-net Furukawa sites), response acceleration was 22m/s$^2$ at 1.2s and 8-16m/s$^2$ at 0.8-1.2s. Similarly the

Table 1 Ground motions

| Earthquakes | Ground motions | PGA ($m/s^2$) | PGV (m/s) | PGD (m) |
|---|---|---|---|---|
| 2011 Great East Japan earthquake | JMA Furukawa | 5.68 | 0.84 | 0.25 |
| | K-net Furukawa | 5.86 | 0.91 | 0.27 |
| | K-net Sendai | 18.0 | 0.83 | 0.25 |
| | K-net Tsukidate | 29.3 | 1.11 | 0.16 |
| 1995 Kobe earthquake | JMA Kobe | 8.91 | 1.05 | 0.30 |
| | JR Takatori | 7.84 | 1.65 | 0.57 |
| 2008 Iwate-Miyagi earthquake | KiK-net Ichinoseki-nishi | 40.2 | 0.98 | 0.31 |

response acceleration was $27m/s^2$ at 0.6s at K-net Sendai. Thus it is considered that response accelerations were quite high at the sites where soils were weak.

This paper tries to evaluate the intensity of ground motions during the 2011 Great East Japan earthquake based on seismic responses of several bridges in comparison with response of the same bridges under ground accelerations during the 1995 Kobe earthquake ($M_{JMA}$7.3, $M_W$6.9) and 2008 Iwate-Miyagi earthquake ($M_{JMA}$7.2, $M_W$6.9). Ground accelerations at JMA Kobe and JR Takatori during the 1995 Kobe earthquake and KiK-net Ichinoseki-nishi during the 2008 Iwate-Miyagi earthquake (refer to Figs. 4 and 5) are used in this study for this purpose. JMA Kobe and JR Takatori ground accelerations are widely used for dynamic response analysis in design of bridges after the 1995 Kobe earthquake. Table 1 summarizes the PGA, PGV and PGD for seven ground motions. Ground velocities and displacements were computed in the frequency domain with a high pass filter of 1/10Hz.

## TARGET BRIDGES

For evaluating the intensity of ground motions among the three earthquakes, response of three target bridges were compared. Though it is preferable to compare responses of various types of bridges, only three span continuous plate girder bridges supported by four reinforced concrete columns and five elastomeric bearings per column are considered as shown in Fig. 6. The bridges supported by 10 m, 15 m and 20 m tall columns are called A-bridge, B-bridge and C-bridge hereinafter. The bridges were in the important bridge category. Basic dimensions of the three bridges were designed based on the design specifications of highway bridges (JRA 2002). Type-II ground condition (moderate soil) was assumed here. It should be noted however that only inelastic static analysis was conducted for deciding dimensions. In real design, linear and nonlinear dynamic response analyses are conducted, but they were not conducted for three target bridges here.

Based on the inelastic static analysis, a part of superstructure supported by a column is analyzed independently with other sections, and this bridge column must satisfy the following requirement.

$$k_{hc}W \le P_a \tag{1}$$

where $P_a$ is lateral capacity of a column, $W$ is tributary weight of a superstructure-column system, and $k_{hc}$ is an equivalent seismic coefficient as

$$k_{hc} = c_z c_s k_{hc0} \ge 0.4 c_z \tag{2}$$

where

$$c_s = 1/\sqrt{2\mu_a - 1} \tag{3}$$

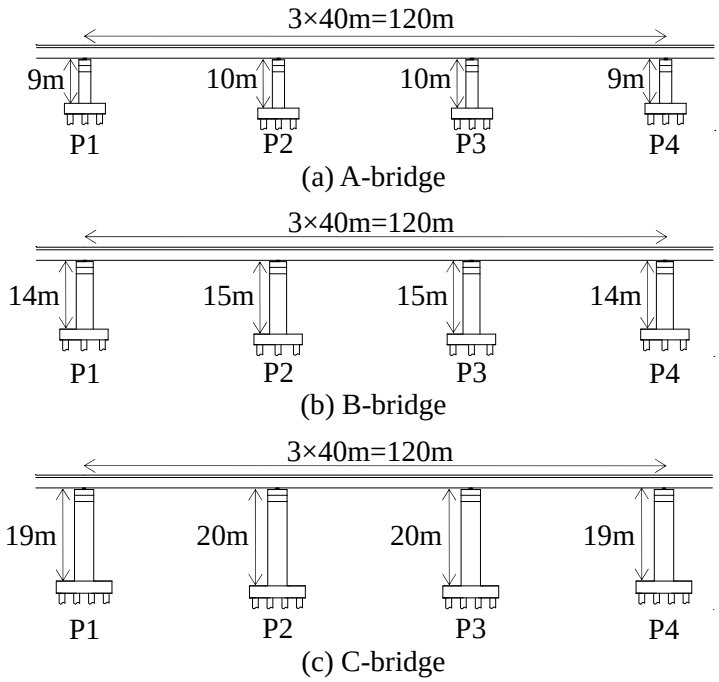


Fig. 6 Target bridges

Table 2 Fundamental natural periods of the target bridges

| | A-bridge | B-bridge | C-bridge |
|---|---|---|---|
| Longitudinal direction | 1.14 s | 1.22 s | 1.25 s |
| Transverse direction | 1.16 s | 1.23 s | 1.29 s |

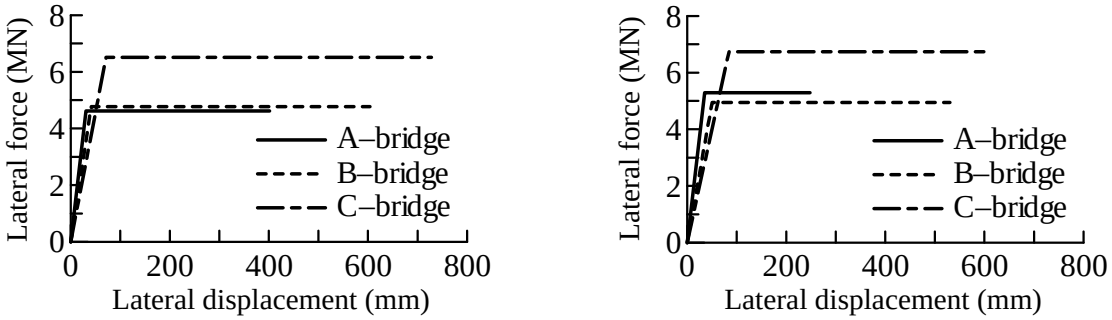


(a) Longitudinal direction (b) Transverse direction

Fig. 7 Lateral force vs. lateral displacement skelton

where $k_{hc0}$ is an elastic lateral seismic coefficient depending on zone, ground condition and the natural period, $c_s$ is structural response modification factor, $\mu_a$ is design displacement ductility factor and $c_z$ is zoning factor (1.0, 0.85 and 0.7 depending on zones).

Several iterations are required in the inelastic static analysis. Table 2 shows the fundamental natural periods of the three bridges thus designed. Since the flexibility of elastomeric bearings predominantly controls the fundamental natural period of the three bridges, the fundamental natural period is close in the three bridges. This is insufficient to evaluate the intensity of ground accelerations, but as a preliminary evaluation, the following analysis was conducted.

The equivalent seismic coefficient $k_{hc0}$ of the three bridges become 1.75 in both the longitudinal and transverse directions. On the other hand, a lateral force vs. lateral displacement skelton was evaluated based on a fiber element analysis as shown in Fig. 7. Thus the column design

Table 3 Determination of $k_{hc}$

| | A-bridge | | B-bridge | | C-bridge | |
|---|---|---|---|---|---|---|
| | LG | TR | LG | TR | LG | TR |
| $k_{hc0}$ | 1.75 | | | | | |
| $u_y$ (mm) | 30.8 | 35.5 | 41.5 | 50.5 | 71.4 | 84.6 |
| $u_u$ (mm) | 401 | 248 | 604 | 530 | 728 | 605 |
| $\mu_a$ | 9.0 | 5.0 | 10.0 | 7.3 | 7.1 | 5.1 |
| $c_s$ | 0.24 | 0.33 | 0.23 | 0.27 | 0.27 | 0.33 |
| $k_{hc}$ | 0.42 | 0.58 | 0.40 | 0.47 | 0.48 | 0.58 |

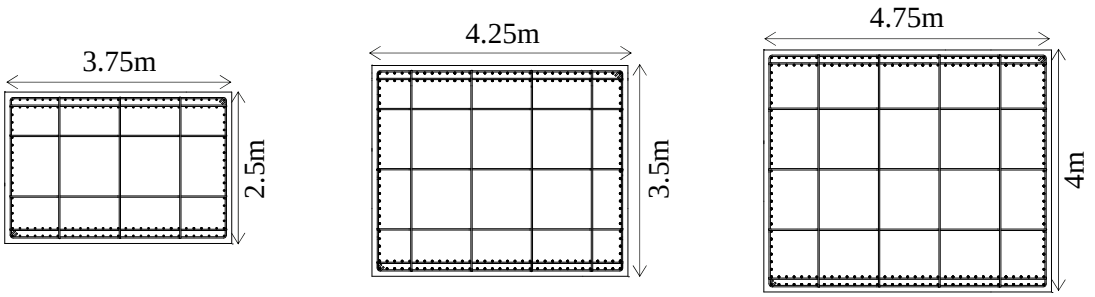


(a) A-bridge (b) B-bridge (c) C-bridge

Fig. 8 Cross section of bridge columns

ductility factor $\mu_a$ was determined as

$$\mu_a = 1 + \frac{u_u - u_y}{\alpha u_y} \tag{4}$$

where $u_y$ and $u_u$ are the yield and ultimate displacements, and $\alpha$ is a safety factor (1.5 for important bridges and 1.2 for less important bridges). Thus, $\mu_a$, $c_s$ and $k_{hc}$ are evaluated as shown in Table 3. It is noted that $k_{hc}$ is in the range of 0.4-0.58 depending on bridges and directions.

Fig. 8 shows the dimensions of columns of three target bridges. Width and depth of the column are 3.75m×2.5m, 4.25m×3.5m and 4.75m×4m for A-, B- and C-bridges, respectively. 29, 32 and 35mm deformed longitudinal bars are set in double in the longitudinal direction, while 22mm deformed tie bars are set at 150mm interval. Cross bars with the same diameters and interval are set inside the core concrete. 135 degree bent hocks are used at both ends of the ties and cross bars.

Pile foundations were designed so that the following requirement is satisfied to mitigate inelastic deformation in piles.

$$k_f \geq (1 + c_p) k_{hc} \tag{5}$$

in which $k_f$ is seismic coefficient for a pile foundation, and $c_p$ is an overstrength factor ($c_p$ = 0.1).

Elastomeric bearings were designed so that the shear deformation of rubber $\gamma_B$ is within the following limit

$$\gamma_B \leq 2.5 \tag{6}$$

where

$$\gamma_B = \frac{u_B}{\Sigma t_e} \tag{7}$$

Table 4 Shear strain of elastomeric bearings in static analysis

| | A-bridge | | B-bridge | | C-bridge | |
|---|---|---|---|---|---|---|
| | LG | TR | LG | TR | LG | TR |
| $k_{hc}$ | 0.42 | 0.58 | 0.40 | 0.47 | 0.48 | 0.58 |
| $u_B$ (mm) | 112 | 153 | 105 | 124 | 126 | 152 |
| $\gamma_B$ (%) | 116 | 160 | 110 | 130 | 132 | 158 |

$$u_B = \frac{k_{hc} W_U}{K_B} \tag{8}$$

in which $u_B$ is lateral displacement of an elastomeric bearing, $\Sigma t_e$ is the total thickness of rubber layers, $W_U$ is a tributary weight of a superstructure, and $K_B$ is lateral stiffness of an elastomeric bearing.

For simplicity of design, it was assumed here that five elastomeric bearings with the same size, thickness and stiffness are used per column in the three bridges. The stiffness of five elastomeric bearings was $2.36\times10^4$kN/m and $7.86\times10^6$kN/m in the lateral and vertical directions, respectively. As mentioned before, this assumption led to the close natural periods in the three bridges. Table 4 summarizes shear strain $\gamma_B$ based on the inelastic static analysis. The size of elastomeric bearings is determined based on static and dynamic response analyses in a real design, however this process was eliminated in this study for simplicity as mentioned before. Thus the real response in the dynamic response analysis under recorded ground accelerations are much larger than $\gamma_B$ shown in Table 4 as will be presented later.

## ANALYTICAL IDEALIZATION

Three bridges were idealized by a three dimensional discrete model in dynamic response analysis. The plastic hinge zone of columns was idealized using fiber elements. Elastomeric bearings and the soil-structure interaction effect were idealized using a set of linear springs. Skelton curve and unloading & reloading hystereses of stress vs. strain relation of confined core concrete was assumed based on Hoshikuma et al (1997) and Sakai and Kawashima (2006). Modified Menegotto-Pinto model (1973) was used to idealize the stress vs. strain hystereses of longitudinal bars.

In the dynamic response analysis, Rayleigh damping was used assuming 2 %, 4% and 20 % for structural components, elastomeric bearings and soils, respectively.

Dynamic response analysis was conducted by imposing the three directional components of the ground motions shown in Figs. 2 and 4. NS, EW and UD components were imposed in the longitudinal, transverse and vertical directions of the bridges.

## SEISMIC RESPONSE OF THREE BRIDGES

As will be described later, since the deck response is generally larger in the longitudinal direction than the transverse direction, the deck response displacement of A-bridge in the longitudinal direction are shown in Fig. 9 for comparison. The deck response displacement at P2 is focused for such a purpose. The peak deck displacement is the largest under JR Takatori acceleration, and it reaches 0.66m which is a quite large value for mitigating damage of expansion joints due to collisions between adjacent decks. This response is also very tough for drivers for controlling automobiles. It is interesting to compare this response to the response under JMA Furukawa acceleration. Both JR-Takatori and JMA Furukawa ground accelerations have nearly 22m/s$^2$ response accelerations at 1.2s which correspond to the fundamental natural period of A-bridge. However the peak deck displacement is 0.46m under JMA

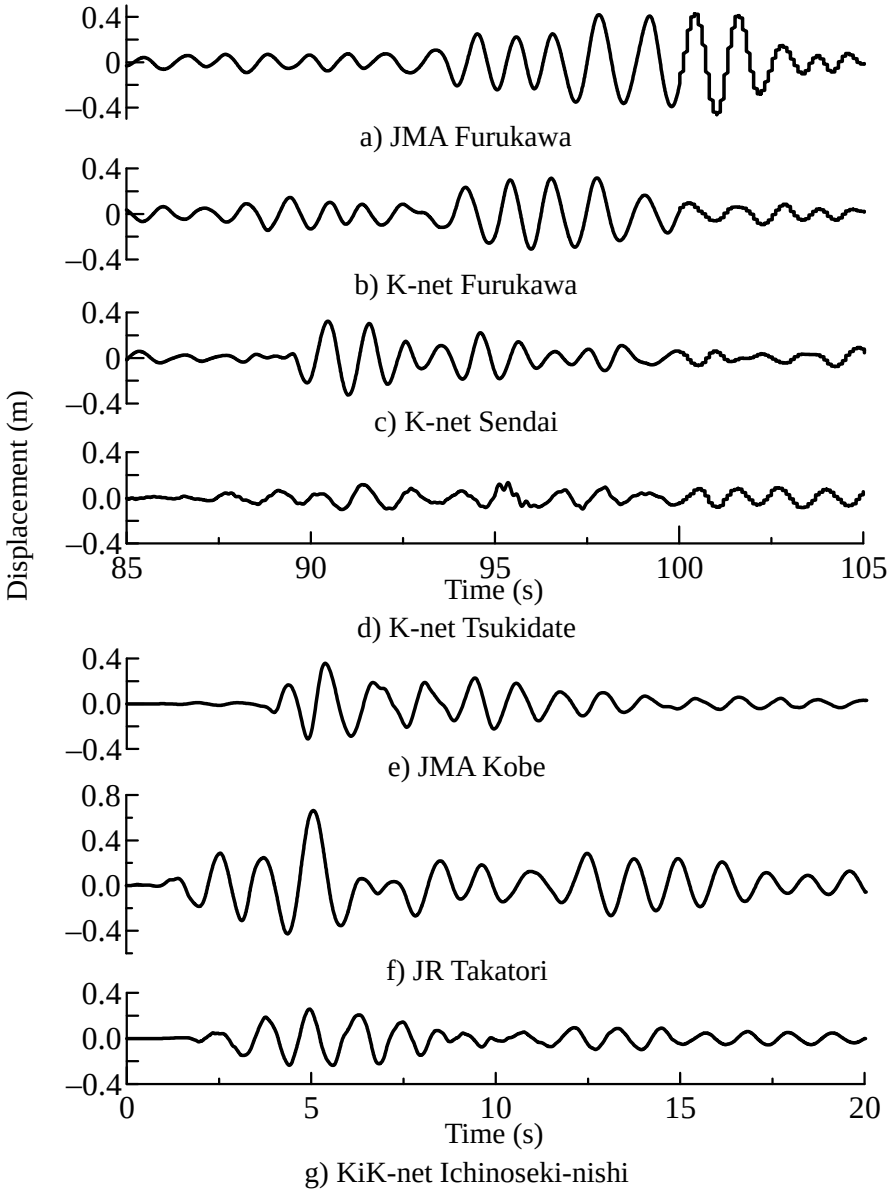


Fig. 9 Deck response displacement at P2 of A-bridge in the longitudinal direction

Furukawa accelerations which is only 70% of the peak deck displacement under JR-Takatori acceleration. Such a point cannot be known from only the comparison of response accelerations.

Obviously the peak deck displacement under K-net Tsukidate ground acceleration is only 0.13m which is much smaller than the peak deck displacement under JMA Furukawa and K-net Furukawa ground accelerations. The peak deck displacement under KiK-net Ichinoseki-nishi record is in a comparative level with the response under K-net Furukawa, K-net Sendai and JMA Kobe records.

Fig. 10 compares lateral force vs. lateral displacement hystereses at the top of P2 for the seven ground accelerations. The response ductility factor $\mu_r$ is defined as

$$\mu_r \equiv \frac{u_{\max}}{u_y} \tag{9}$$

where $u_{\max}$ and $u_y$ are the peak displacement and yield displacement at the top of column. The response ductility factor $\mu_r$ is the largest ($\mu_r$ =5.1) under the JMA Furukawa record, but much

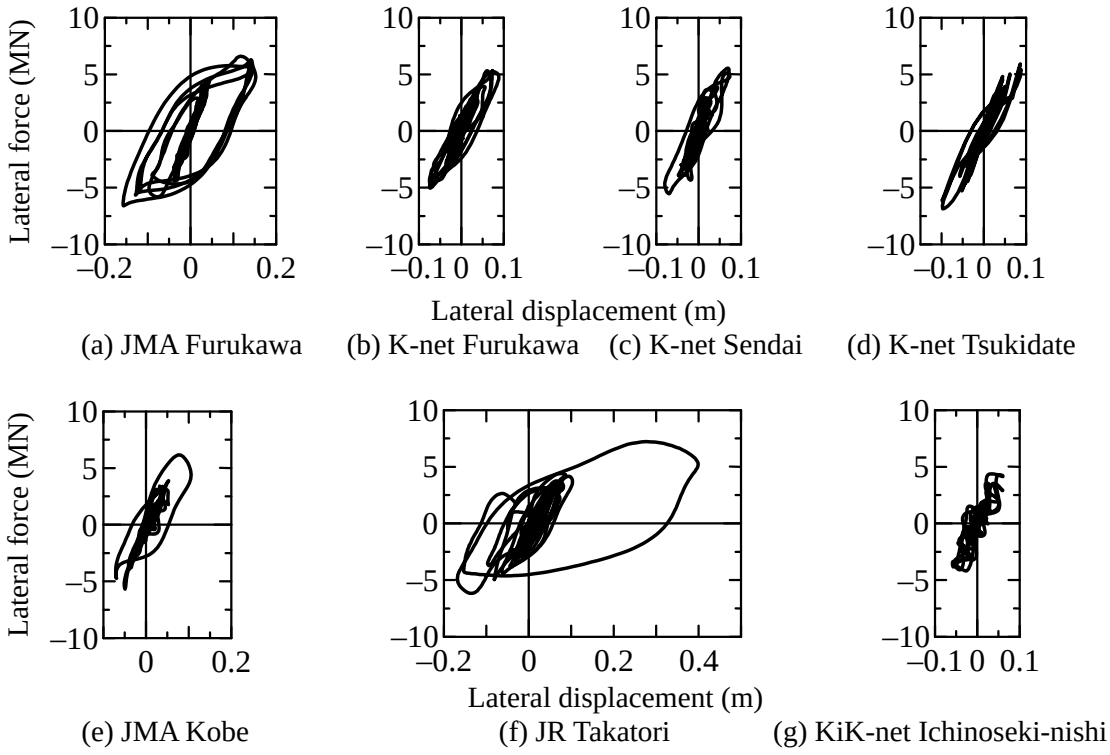


Fig. 10 Force vs. lateral displacement hystereses at the top of P2 column of A-bridge in the longitudinal direction

Table 5 Response ductility factors of P2 column

| Earthquakes | Ground motions | A-bridge | | B-bridge | | C-bridge | |
|---|---|---|---|---|---|---|---|
| | | LG | TR | LG | TR | LG | TR |
| 2011 Great East Japan earthquake | JMA Furukawa | 5.1 | 1.7 | 4.2 | 1.1 | 3.0 | 1.0 |
| | K-net Furukawa | 2.9 | 2.4 | 2.3 | 1.8 | 1.5 | 1.6 |
| | K-net Sendai | 2.6 | 0.9 | 2.3 | 0.8 | 1.5 | 0.7 |
| | K-net Tsukidate | 3.2 | 1.0 | 2.8 | 0.8 | 1.7 | 0.7 |
| 1995 Kobe earthquake | JMA Kobe | 3.4 | 1.4 | 2.6 | 0.9 | 2.3 | 0.9 |
| | JR Takatori | 12.9 | 5.8 | 7.0 | 3.5 | 6.6 | 3.3 |
| 2008 Iwate-Miyagi earthquake | KiK-net Ichinoseki-nishi | 2.0 | 1.3 | 2.5 | 1.2 | 1.5 | 1.0 |

larger $\mu_r$ (=12.9) develops under JR Takatori ground accelerations. The column response ductility factors have the similar trend with that of the peak deck displacement.

Table 5 summarizes the column response ductility factors of the three bridges subjected to seven ground accelerations. Note that response ductility factors $\mu_r$ by Eq. (9) are much smaller than the design ductility factor $\mu_a$ by Eq. (4) (refer to Table 3). In particular, $\mu_r$ in the transverse direction is generally very small except $\mu_r$ evaluated for JR Takatori ground acceleration showing that columns behave almost linearly. Column response ductility factor is the largest under JMA Furukawa ground acceleration among the four ground accelerations recorded during the 2011 Great East Japan earthquake, however the largest column response ductility factor under JMA Furukawa ground acceleration is smaller than the response ductility factor under JR Takatori ground acceleration recorded during the 1995 Kobe earthquake. The similar results are obtained in B- and C-bridges.

Table 6 summarizes the peak shear strain of rubber layers in elastomeric bearings. Again in this case, shear strain computed by dynamic response analysis is much larger than the shear strain evaluated by static analysis (refer to Table 4). As mentioned earlier, in a real design, the elastomeric

Table 6 Peak shear strain of elastomeric bearing on P2 column

| Earthquakes | Ground motions | A-bridge | | B-bridge | | C-bridge | |
|---|---|---|---|---|---|---|---|
| | | LG (%) | TR (%) | LG (%) | TR (%) | LG (%) | TR (%) |
| 2011 Great East Japan earthquake | JMA Furukawa | 295 | 186 | 341 | 175 | 327 | 216 |
| | K-net Furukawa | 233 | 361 | 231 | 319 | 247 | 340 |
| | K-net Sendai | 246 | 148 | 247 | 149 | 287 | 177 |
| | K-net Tsukidate | 182 | 136 | 165 | 119 | 132 | 112 |
| 1995 Kobe earthquake | JMA Kobe | 268 | 213 | 279 | 190 | 305 | 206 |
| | JR Takatori | 316 | 351 | 415 | 395 | 336 | 301 |
| 2008 Iwate-Miyagi earthquake | KiK-net Ichinoseki-nishi | 191 | 225 | 242 | 196 | 237 | 175 |

bearings have to be re-sized based on the computed shear deformation by dynamic response analysis, however this process was eliminated in this study for simplicity. The general trend of the dependence of ground accelerations is similar with the above results. JR Takatori accelerations results in the largest shear strain in the elastomeric bearings followed by JMA Furukawa ground accelerations.

## CONCLUSIONS

In this study, impacts of the ground motions recorded at soft soil sites during the 2011 Great East Japan earthquake was evaluated in comparison with JMA Kobe and JR Takatori ground accelerations which are widely used for dynamic response analysis in design. A ground acceleration recorded at KiK-net Ichinoseki-nishi during the 2008 Iwate-Miyagi earthquake was also included in analysis for comparison. Based on the results presented herein, the following conclusions may be deduced:

1) Most of ground accelerations recorded at K-net and JMA net were recorded at stiff sites. Thus PGA and response accelerations at period shorter than 0.3s was extremely high, however it develops only small response in the target bridges.

2) In particular, a ground acceleration at K-net Tsukidate had an extremely high PGA of 27m/s$^2$ and high response acceleration of 129m/s$^2$ at 0.24s, but it develops very small response in the target bridges. This clearly explains the fact that the structural damage in Tsukidate during the 2011 Great East Japan earthquake was minor though JMA intensity was 7.

3) On the other hand, a ground acceleration recorded at JMA Furukawa develops much larger response in the target bridges than the ground acceleration recorded at Tsukidate. However the response of the target bridges under JMA Furukawa ground acceleration is smaller than that under JR Takatori acceleration recorded during the 1995 Kobe earthquake. Since the type II design response spectra were determined based on the ground motions developed during the 1995 Kobe earthquake, it is considered that the ground motions recorded at K-net and JMA-net during the 2011 Great East Japan earthquake was smaller than the Type II design spectra. This is a major contribution to the fact that the bridges which were designed in accordance with the post-1990 design codes suffered almost no damage during the 2011 Great East Japan earthquake.

4) A ground acceleration recorded at KiK-net Ichinoseki-nishi during the 2008 Iwate-Miyagi earthquake develops similar or slightly smaller response in the target bridges than JMA Kobe ground acceleration recorded during the 1995 Kobe earthquake.

5) Since computed nonlinear response of the target bridges exhibits responses which are different from expected response assessed based on only response spectra, it is important to evaluate intensity of ground motions based on nonlinear response of several target bridges with different structural properties. By identifying several bridges as target bridges among researchers, response comparison of

several target bridges can be a useful measure to evaluate the intensity of various ground motions.

## ACKNOWLEDGMENTS

The authors would like to acknowledge the National Research Institute for Earth Science and Disaster Prevention, and Japan Meteorological Agency for providing strong ground motion records used in this study.

## REFERENCES

Hoshikuma, J., Kawashima, K. and Taylor, A. W. (1997). "Stress-strain model for confined reinforced concrete in bridge piers." *Journal of Structural Engineering*, ASCE, Vol. 123, No. 5, 624-633.

Japan Road Association (1996, 2002). "Design specifications of highway bridges - Part V Seismic design." Maruzen, Tokyo, Japan.

Japan Society of Civil Engineers (2011). "Reconnaissance damage investigation for the 2011 Great East Japan earthquake." Earthquake Engineering Committee, Tokyo, Japan.

Kawashima, K. (2000). "Seismic design and retrofit of bridges." Key note presentation, *12th World Conference on Earthquake Engineering*, 1-20, Paper No. 1818, Auckland, New Zealand.

Kawashima, K. (2012). "Damage of bridges due to the 2011 Great East Japan earthquake." *Proc. International Symposium on Engineering Lessons Learned from the 2011 Great East Japan Earthquake*, Japan Association for Earthquake Engineering, Architectural Institute of Japan, Japan Society of Civil Engineers, Japanese Geotechnical Society, Japan Society of Mechanical Engineers, and Seismological Society of Japan, Tokyo, Japan.

Menegotto, M. and Pint, P. E. (1973). "Method of analysis for cyclically loaded RC plane frames including changes in geometry and non-elastic behavior of elements under combined normal force and bending." *Proc. IABSE Symposium on Resistance and Ultimate Deformability of Structures Acted by Well Defined Repeated Loads*, 15-22.

Sakai, J. and Kawashima, K. (2006). "Unloading and reloading stress-strain model for confined cncrete." *Journal of Structural Engineering*, ASCE, Vol. 132, No. 1, 112-122.